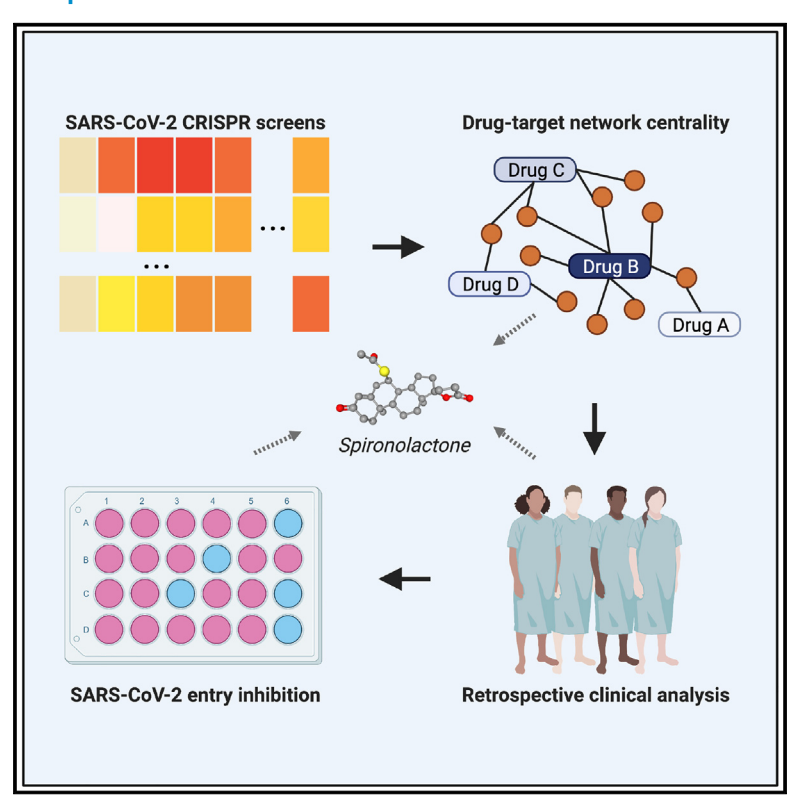


# Integrative analysis of functional genomic screening and clinical data identifies a protective role for spironolactone in severe COVID-19

# **Graphical abstract**



# **Authors**

Henry C. Cousins, Adrienne Sarah Kline, Chengkun Wang, ..., Russ B. Altman, Yuan Luo, Le Cong

# Correspondence

cousinsh@stanford.edu (H.C.C.), russ.altman@stanford.edu (R.B.A.), yuan.luo@northwestern.edu (Y.L.), congle@stanford.edu (L.C.)

# In brief

Cousins et al. demonstrate a network-based method for prioritizing drug candidates based on functional genomics screens. Using this approach and follow-up with both retrospective clinical analysis and *in vitro* viral infection assays, they identify the potassium-sparing diuretic spironolactone as a potential modulator of SARS-CoV-2 entry.

# **Highlights**

- RxGRID is a method for network-based drug prioritization using CRISPR screening data
- RxGRID identifies spironolactone as a potential modulator of SARS-CoV-2 entry
- Spironolactone is associated with improved COVID-19 outcomes in a retrospective study







# Report

# Integrative analysis of functional genomic screening and clinical data identifies a protective role for spironolactone in severe COVID-19

Henry C. Cousins, <sup>1,2,\*</sup> Adrienne Sarah Kline, <sup>3</sup> Chengkun Wang, <sup>4,5</sup> Yuanhao Qu, <sup>4,5</sup> James Zengel, <sup>5,6</sup> Jan Carette, <sup>5,6</sup> Mengdi Wang, <sup>7</sup> Russ B. Altman, <sup>1,4,8,9,\*</sup> Yuan Luo, <sup>3,\*</sup> and Le Cong<sup>4,5,10,\*</sup>

https://doi.org/10.1016/j.crmeth.2023.100503

**MOTIVATION** The emergence of SARS-CoV-2 variants with resistance to existing COVID-19 treatments and evasion from prior vaccination reinforces the need for drugs targeting host entry factors. Nonetheless, there is a lack of methods that systematically and rapidly prioritize host-targeting drugs for viral infection. High-throughput functional screens provide an unbiased and broadly accessible means of identifying genes that influence the infection of host cells. However, it remains challenging to infer pharmacologic signatures from functional screening data.

# **SUMMARY**

We demonstrate that integrative analysis of CRISPR screening datasets enables network-based prioritization of prescription drugs modulating viral entry in severe acute respiratory syndrome coronavirus 2 (SARS-CoV-2) by developing a network-based approach called Rapid proXimity Guidance for Repurposing Investigational Drugs (RxGRID). We use our results to guide a propensity-score-matched, retrospective cohort study of 64,349 COVID-19 patients, showing that a top candidate drug, spironolactone, is associated with improved clinical prognosis, measured by intensive care unit (ICU) admission and mechanical ventilation rates. Finally, we show that spironolactone exerts a dose-dependent inhibitory effect on viral entry in human lung epithelial cells. Our RxGRID method presents a computational framework, implemented as an open-source software package, enabling genomics researchers to identify drugs likely to modulate a molecular phenotype of interest based on high-throughput screening data. Our results, derived from this method and supported by experimental and clinical analysis, add additional supporting evidence for a potential protective role of the potassium-sparing diuretic spironolactone in severe COVID-19.

# **INTRODUCTION**

Host cell entry represents a critical stage of the severe acute respiratory syndrome coronavirus 2 (SARS-CoV-2) replication cycle that determines the tropism and virulence of emerging variants. SARS-CoV-2 entry relies canonically on binding between viral spike protein and host ACE2, as well as processing of the spike

protein by endogenous proteases, most notably TMPRSS2 and furin.<sup>2,3</sup> However, the complete entry process relies both directly and indirectly on a network of hundreds of host genes that remains poorly understood.<sup>4,5</sup>

Heterogeneity in expression patterns of accessory entry factors, which facilitate viral adhesion, cleavage events, and membrane fusion, is a chief determinant of viral susceptibility in terms



<sup>&</sup>lt;sup>1</sup>Department of Biomedical Data Science, Stanford University School of Medicine, Stanford, CA 94305, USA

<sup>&</sup>lt;sup>2</sup>Medical Scientist Training Program, Stanford University School of Medicine, Stanford, CA 94305, USA

<sup>&</sup>lt;sup>3</sup>Department of Preventive Medicine, Feinberg School of Medicine, Northwestern University, Chicago, IL 60611, USA

<sup>&</sup>lt;sup>4</sup>Department of Pathology, Stanford University School of Medicine, Stanford, CA 94305, USA

<sup>&</sup>lt;sup>5</sup>Department of Genetics, Stanford University School of Medicine, Stanford, CA 94305, USA

<sup>&</sup>lt;sup>6</sup>Department of Microbiology and Immunology, Stanford University School of Medicine, Stanford, CA 94305, USA

<sup>&</sup>lt;sup>7</sup>Department of Electronic Engineering, Princeton University, Princeton, NJ 08544, USA

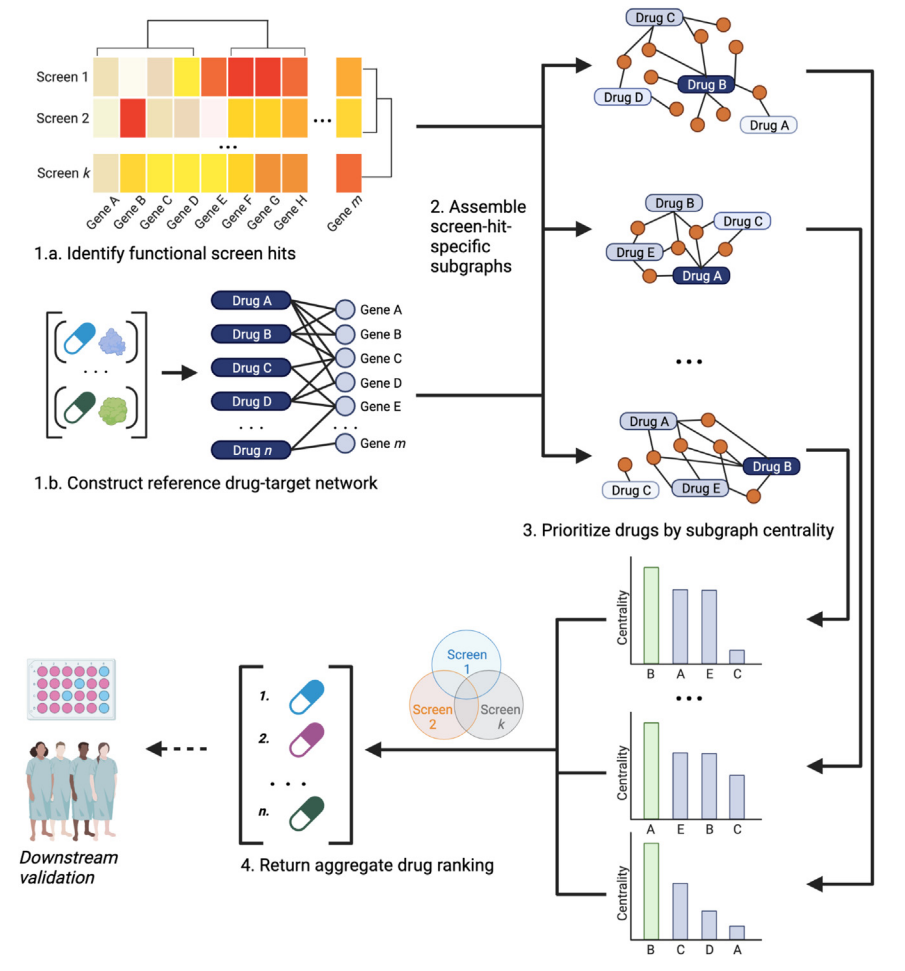
<sup>&</sup>lt;sup>8</sup>Department of Medicine, Stanford University School of Medicine, Stanford, CA 94305, USA

<sup>&</sup>lt;sup>9</sup>Department of Bioengineering, Stanford University, Stanford, CA 94305, USA

<sup>&</sup>lt;sup>10</sup>Lead contact

<sup>\*</sup>Correspondence: cousinsh@stanford.edu (H.C.C.), russ.altman@stanford.edu (R.B.A.), yuan.luo@northwestern.edu (Y.L.), congle@stanford.edu (L.C.)





of both tissue types and patient subgroups.<sup>6,7</sup> Consequently. drug interactions with such host factors can promote or inhibit viral entry in vitro and have, in certain, subgroups demonstrated clinical benefit in large-scale studies.8-10 With the emergence of SARS-CoV-2 variants with significant genome-wide mutational load, therapeutics and vaccines targeting viral proteins of early strains have shown reduced efficacy in recent outbreaks. 11-13 Further, structural and functional study of the Omicron mutational landscape revealed a range of adaptive mutations that facilitate escape from antibody neutralization and vaccine protection while preserving high-affinity viral interactions with host receptor. 12,14,15 There consequently exists a pressing need to identify therapies that modulate host entry factors, which may be both more robust to future variants and complementary to existing direct-acting antivirals such as nirmatrelvir and molnupiravir. 16,17

High-throughput functional genetic screens, primarily performed with CRISPR-Cas9 systems in knockout (CRISPR-KO) and activation (CRISPRa) formats, provide a powerful tool to identify host genes that facilitate viral entry. 18-25 Such methods enable causal inference of single-gene effects that may be confounded in gene expression assays by both epistatic patterns and immune mechanisms distinct from viral entry. CRISPR screens can also quantify gene effects in distinct cell types and different perturba-

# Figure 1. Integrated analysis of SARS-CoV-2 entry networks for drug repositioning

In RxGRID, functional genetic hits for a phenotype of interest are first obtained from one or more screens. These are combined with drug-target interactions from DrugBank to generate drug-gene subnetworks for hit genes from each screen. In parallel, drugs are prioritized based on normalized degree centrality within each subnetwork, and top drugs are defined based on mutual overlap among screens. Top drugs may then be validated in additional downstream analysis, such as targeted inhibition assays or retrospective cohort studies.

tion schemas, which provide specific mechanistic insights but can limit the generalizability of findings from any individual experiment.26

We hypothesized that integrated analysis of multiple viral-entry functional screens would reveal a shared network of host entry genes with more generalizable implications for drug repurposing than would be possible using individual datasets. We performed drug-target network analysis using all publicly available, genome-wide CRISPR screens of SARS-CoV-2 viral entry, which identified three common drugs, spironolactone, carvedilol, and quetiapine, as potential modulators of viral entry. Furthermore. we conducted a retrospective clinical outcome analysis of these drugs using medical records from 64,349 COVID-19 patients, which supported a significant

protective role for spironolactone. Finally, we demonstrated that spironolactone exerts a time-dependent inhibitory effect on SARS-CoV-2 viral entry in human lung cells, suggesting that spironolactone may mediate a milder disease course by suppressing viral entry.

### **RESULTS**

To identify host subnetworks that facilitate SARS-CoV-2 viral entry (Figure 1), we obtained genome-wide CRISPR screens measuring the impact of individual genes' expression on viral infection in human cells. The screens accounted for a variety of cellular contexts, including both lung and non-lung cell types, and functional perturbations, namely loss-of-function (i.e., CRISPR-KO) and increaseof-expression (i.e., CRISPRa) screens (Table S1). The final dataset collection included five CRISPR-KO and three CRISPRa screens, enabling resolution of context-dependent entry mechanisms that could not be identified by only the KO datasets.

The eight screens exhibited variable levels of correlation at the single-gene level, consistent with their heterogeneous cellular contexts (Figure 2A). 88% (7/8) of screens were significantly correlated with at least one other screen, while 32% (9/28) of all pairwise comparisons revealed a significant positive





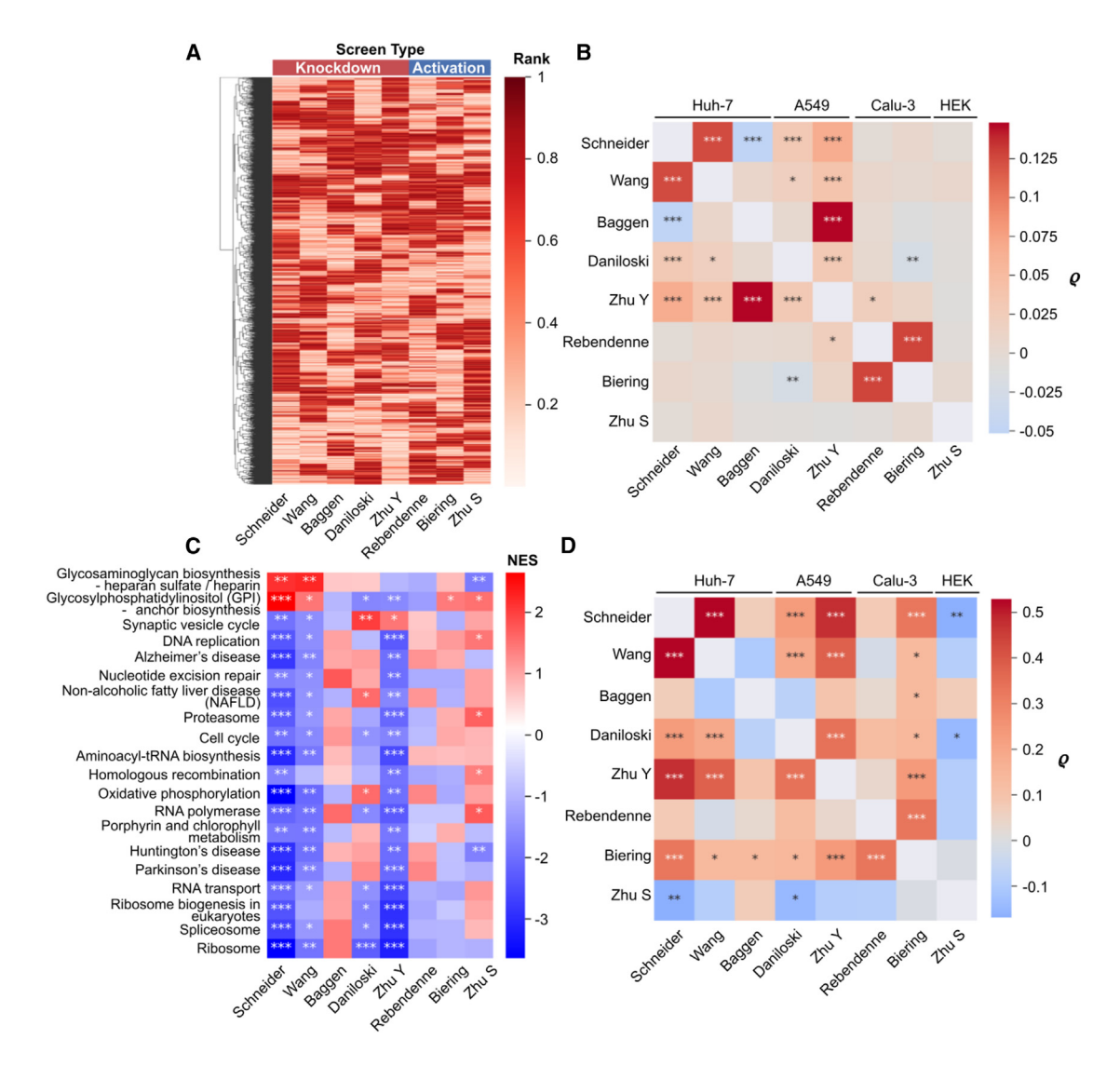


Figure 2. Correlations and functional enrichment patterns among screens demonstrate significant variations, requiring RxGRID for crossscreen integration and interpretation

(A) Cluster map of individual gene ranks for all screens. Red bars indicate knockdown screens, and blue bars indicate activation screens.

(B) Pairwise correlation measurements among screens. Annotations indicate significance at the nominal level (\*), after correcting for multiple testing among screens (\*\*), and after correcting for multiple testing among all pairs (\*\*\*). A majority of knockdown screens demonstrate correlation at a nominal or higher significance.

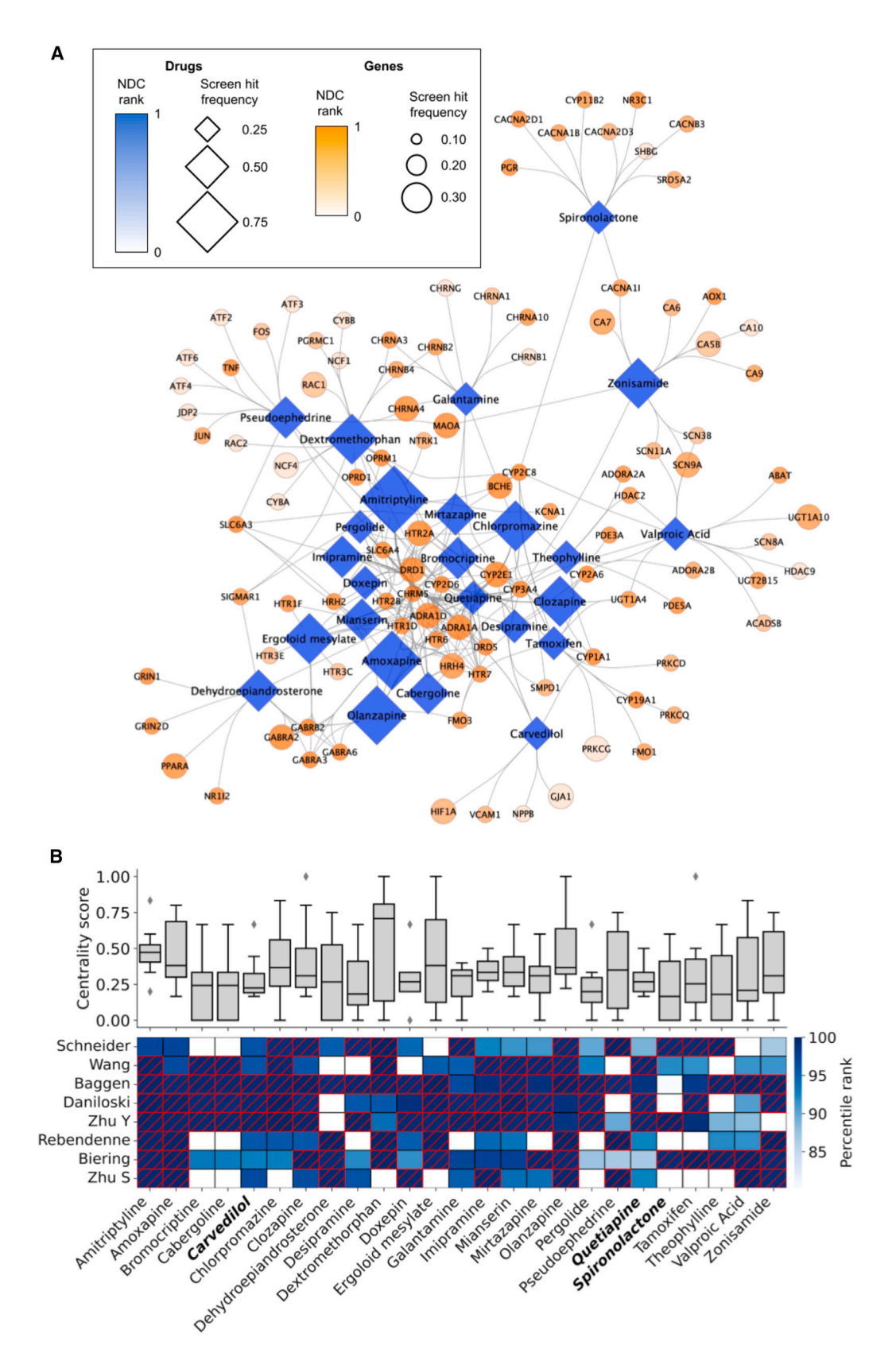
(C) Pathways with significant enrichment in multiple screens involve cellular adhesion and synaptic transport. Annotations indicate significance at false discovery rate (FDR) values of 0.4 (\*), 0.05 (\*\*), and 0.001 (\*\*\*).

(D) Interscreen correlations for KEGG pathway enrichment scores are stronger than for individual gene scores. Annotations are the same as in (B).

correlation (Figure 2B). Gene-level agreement was higher within each class of screen, with a significant positive correlation among 70% (7/10) of CRISPR-KO and 33% (1/3) of CRISPRa screen pairs. Both pairs of screens performed in lung-derived tissue were significantly positively correlated at the single-gene level, although cellular context was not significantly associated with gene-level correlation overall.

We next quantified functional pathway enrichment among each screen using gene set enrichment analysis. 20 KEGG pathways were significantly enriched in at least two screens, including several pathways with known involvement in SARS- CoV-2 entry (Figure 2C). Pathways involved in glycosaminoglycan and phosphoglyceride production were most strongly enriched, consistent with their essential role in viral attachment.<sup>27</sup> We also observed significant de-enrichment of pathways involved in neurodegenerative disease, including Alzheimer's, Huntington's, and Parkinson's diseases, as well as synaptic signaling broadly. Correlations among normalized pathway enrichment scores for each screen were generally higher than correlations for individual genes, although screens with higher gene-level correlations tended to have higher pathway correlations as well (Figure 2D).





Report



We next constructed unweighted networks representing known interactions between existing drugs and entry genes identified in individual screens (Figure 3A). Each network contained an average of 117 (standard deviation 8.86) genes, 608 (210) drugs, and 773 (334) edges each, corresponding to an average density of 1.07% (0.118%). The mean degree of each graph was 6.63 (2.90) for gene nodes, 1.24 (0.105) for drug nodes, and 2.07 (0.257) overall.

We prioritized drugs for downstream analysis based on centrality within each hit network. As both local (normalized degree centrality [NDC]) and global (betweenness) measures of centrality yielded similar rankings ( $\rho$  = 0.99, p < 0.001), we used NDC for subsequent analyses due to its interpretability. No drug met significance in all screens, while 209 drugs were significant in at least one dataset (Figure S1). 25 drugs met significance in at least three datasets (Figure 3B). Drug hits encompassed a range of functional categories, with a predominance of ion-channeltargeting compounds. Tricyclic antidepressants were the most common category, comprising 20% (5/25) of hits, followed by dopamine agonists and atypical antipsychotics, both of which comprised 12% (3/25).

We next performed a propensity-score-matched (PSM) retrospective clinical analysis to evaluate whether use of candidate drugs was associated with COVID-19 disease severity (Figures 4A and S2). We obtained electronic medical records from a large academic hospital system, which yielded 64.349 patient records with a positive COVID-19 test. Of the drugs meeting centrality significance, only three medications had a sufficient treatment cohort size for PSM analysis: carvedilol, quetiapine, and spironolactone (Figure 4B). Additionally, we included metformin as a comparative control, as it has a negative association with COVID-19 severity reproduced in a variety of clinical studies.9,28-31

We observed a significant negative association between spironolactone use and progression to intensive care unit (ICU) admission (odds ratio [OR] 0.34;  $Cl_{95}$  0.17-0.68; p = 0.002). The association between spironolactone use and progression to mechanical ventilator status was also significantly negative (OR 0.19;  $Cl_{95}$  0.055–0.645; p = 0.006). The comparator, metformin, also exhibited a significant negative association with progression to ICU admission (OR 0.49; Cl<sub>95</sub> 0.35-0.68; p < 0.001) and a nominally significant association with progression to mechanical ventilator status (OR 0.50;  $Cl_{95}$  0.29-0.85; p = 0.014), consistent with the secondary findings of the COVID-OUT randomized controlled trial.31 We did not observe a significant association with progression to either ICU admission or mechanical ventilator status for either carvedilol or quetiapine following multiple hypothesis correction.

Given that spironolactone use was associated with a significant reduction in risk of severe COVID-19 in our cohort analysis, we evaluated whether its mechanism could be mediated by inhibition of viral entry. We performed a SARS-CoV-2 virus entry assay in a human lung epithelial cell line, alongside a rabies virus (RABV) control. Across varying doses of spironolactone, we observed a time- and dose-dependent drug inhibitory effect on viral entry (Figure 4C), with a strong negative correlation between spironolactone dose and infected cell count, amounting at the highest dose to a 68% reduction in infected cell levels (p < 0.001; Figure 4D). Further, the parallel RABV control did not show an equivalent effect, confirming that this spironolactone inhibition is specific to SARS-CoV-2 spike-mediated entry (Figures 4E and 4F). We observed a similar inhibitory effect for spironolactone in a separate, non-lung cell line, where there was again a significant decrease in infected cell levels for increasing doses of spironolactone, amounting to a 14% reduction in infected cell levels at the highest dose (p = 0.002; Figure S4).

# **DISCUSSION**

Our analysis demonstrates that genome-wide CRISPR screens provide a basis for systematic prioritization of drug candidates in COVID-19, many of which are not evident in methods reliant on gene expression studies or association hits alone. We identify three common medications, spironolactone, quetiapine, and carvedilol, as potential modulators of SARS-CoV-2 infection based on their interactions with host entry factors. We perform a propensity-score-matched, retrospective cohort study of clinical outcomes for COVID-19 patients on these medications, showing that spironolactone use is associated with reduced likelihood of ICU admission. We further show that spironolactone inhibits SARS-CoV-2 pseudoviral entry in a human lung epithelial cell line in a dose-dependent manner, providing a potential mechanism for the observed therapeutic effect.

Functional genomic screens enable measurement of the effect of individual host genes on viral entry, but their noise levels and context dependence can limit direct clinical applicability. We addressed this barrier by combining data from multiple genomewide CRISPR screens across several experimental and cellular contexts, inferring drug activity based on an abundance of known drug targets among hits, and selecting drugs with high representation among screens for follow-up analysis. Such a prioritization method benefits from direct biological interpretability, as top candidate drugs modulate large numbers of entry factors while enabling higher sensitivity for detecting potential effects. Our method, based on the principle that centrality with respect to hit genes implies pharmacologic relevance, provides unique advantages compared with existing methods. Physics-guided approaches, such as quantitative structure-activity relationship (QSAR) and similarity ensemble approach (SEA), generally apply

## Figure 3. Network-based prioritization of candidate drugs using RxGRID

(A) Summary network after performing RxGRID, showing overlap among the individual screen networks. Drug and gene nodes are labeled by centrality and by the frequency at which they were labeled a hit in individual screens. Psychotropic drugs, particularly tricyclic antidepressants and atypical antipsychotics, show high aggregate centrality, while calcium and potassium channels represent highly targeted entry genes.

(B) Aggregate ranking of candidate drugs. Bars indicate normalized centrality across all screens. Heatmap shows percentile rank in each screen. Red boxes indicate screens in which the given drug was labeled as significant, and bold text indicates drugs with sufficient representation for retrospective clinical investigation.



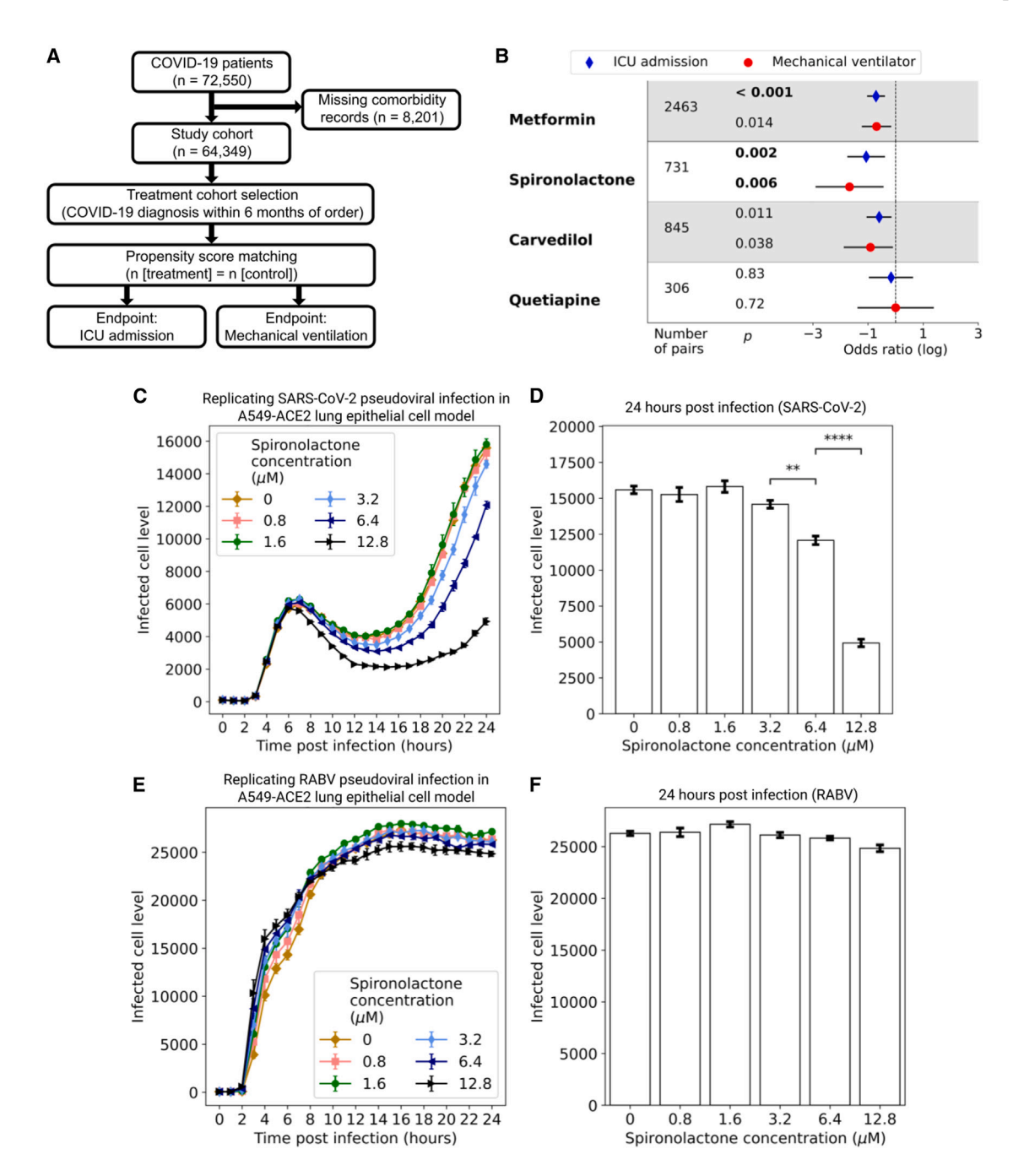


Figure 4. Retrospective clinical validation, coupled with a cell-based drug inhibition assay, provides real-world validation and a mechanistic view on the effects of candidate antiviral drugs

(A) Study design. Propensity-score-matched treatment and control groups were defined for each drug of interest in patients with a COVID-19 diagnosis. Clinical endpoints were ICU admission and mechanical ventilation.

(B) Cohort sizes, odds ratios, and significance levels for individual drugs and endpoints. Bold text indicates drug-endpoint combinations that were significant after Bonferroni correction (a = 0.05; n = 8). Statistically significant negative associations with ICU admission were observed for both spironolactone and metformin, which was included as a comparative control.

(C) Infected cell density over time at increasing doses of spironolactone using replicating SARS-CoV-2 pseudoviral particles in lung epithelial cell line A549-ACE2 (A549 cells expressing human ACE2; n = 3 replicates).

(legend continued on next page)

Report



once a single protein of interest has been identified, which is not feasible for large datasets like CRISPR screens and precludes consideration of effects among target ensembles. 32,33 Enrichment methods, including gene set enrichment analysis (GSEA) and gene set proximity analysis (GSPA), generally rely on biologically motivated null distributions that render the resulting analysis more specific at the expense of sensitivity and may also be vulnerable to experimental noise. 34,35 By representing screen collections as subgraphs within a drug-target network, RxGRID (Rapid proXimity Guidance for Repurposing Investigational Drugs) avoids such issues and enables rapid prioritization of drugs likely to modulate a common phenotype among multiple functional screens. While differences in data requirements and intended use case make direct comparison of such methods challenging, we note that future efforts to compare drug prediction methods for functional genomics data might find our method useful as a benchmark.

Pharmacologic antagonists of the renin-angiotensin-aldosterone system (RAAS), such as spironolactone, have been proposed as potential inhibitors of SARS-CoV-2 infection due to their role as indirect modulators of ACE2 expression. 36,37 For instance, spironolactone has been observed to decrease expression of soluble ACE2, which can promote viral endocytosis, while simultaneously increasing activity of the membrane-associated form. 38-40 Its antiandrogenic action may also decrease expression of TMPRSS2, leading to impaired spike protein proteolysis and activation.<sup>41</sup> Finally, given that COVID-19 is strongly associated with both hypokalemia and hypocalcemia, RAAS antagonists that maintain cation homeostasis, such as spironolactone, may mitigate both ion-channel-mediated viral entry and the clinical sequelae of associated electrolyte imbalances. 42,43 We note that, excluding the cytochrome P450 family, all spironolactone-targeted entry factors in our analysis classify as either androgen signaling proteins or voltage-gated cation channels, supporting a possible combination of mechanisms. Further studies in relevant cell or tissue contexts could help to elucidate the physiological role of these putative host factors and pathways during viral infection.

Despite a variety of mechanistic hypotheses, few investigations of either clinical efficacy or in vitro effect have been performed for spironolactone in COVID-19. A recent interventional study of spironolactone-sitagliptin combination therapy in 263 patients showed statistically non-significant improvements in clinical outcomes, including mortality, ICU admission, intubation rate, and end-organ damage, for patients on spironolactone.<sup>44</sup> Another interventional trial of 55 patients showed lower mortality for COVID-19 patients on potassium canrenoate, a mineralocorticoid receptor antagonist similar to spironolactone, although this also did not reach statistical significance. 45 However, both studies were conducted in small cohorts and may have been underpowered to detect an effect. Our retrospective study design enables both the analysis of a substantially larger treatment cohort and the study of dosing prior to infection.

In addition to spironolactone, RxGRID also prioritized ion-channel-targeting drug classes, such as tricyclic antidepressants and atypical antipsychotics, as potential modulators of viral entry. This is consistent with both previous observational studies of such drugs and the putative role that cation channels, such as membrane-associated calcium and voltage-gated potassium channels, may play in viral entry. 46-49 We also note that, as mentioned previously, network-centrality-based methods such as RxGRID may tend to favor drugs with non-specific protein interactions, which includes many psychoactive medications.

Collectively, our results provide a generalizable method, RxGRID, for applying functional genomics data, such as CRISPR screens, in drug repurposing efforts. The method benefits from relative simplicity and mechanistic interpretability, increasing its value to genomics researchers. Our in vitro experiments and clinical investigation provide compelling evidence for a potential protective role of spironolactone in severe COVID-19, strongly warranting a large-scale randomized controlled trial to resolve this timely and high-impact proposition.

## Limitations of the study

Our study has several limitations, including the use of a single healthcare system (across 11 hospitals) for clinical analysis and the use of pseudotyped virus for validation. It is further important to note that observational drug associations do not necessarily imply causal therapeutic roles, owing both to the necessary presence of unmodeled confounders and to practical restrictions on prescription of the drug of interest, such as safety or cost. Further investigations, including detailed mechanistic analysis and well-powered randomized controlled trials, including specific subgroup analyses by demographic factors, will be necessary to determine any potential therapeutic role for spironolactone in COVID-19.

## **STAR**\*METHODS

Detailed methods are provided in the online version of this paper and include the following:

- KEY RESOURCES TABLE
- RESOURCE AVAILABILITY
  - Lead contact
  - Materials availability
  - Data and code availability
- EXPERIMENTAL MODEL AND STUDY PARTICIPANT DE-TAILS
  - Cell lines
  - Medical records
- METHOD DETAILS
  - O CRISPR screening data
  - Functional enrichment analysis
  - Network-based drug rankings

<sup>(</sup>D) Cell density at increasing doses of spironolactone at 24 h post-infection, showing significant inhibition at higher doses. Brackets show all significant sequential

<sup>(</sup>E) Infected cell density over time at increasing doses of spironolactone using replicating rabies viral particles as a control (n = 3 replicates).

<sup>(</sup>F) Cell density at increasing doses of spironolactone at 24 h post-infection, showing no inhibition at higher doses for the rabies control. Data are represented as mean ± standard error.



- Cohort construction
- Propensity score matching
- Software
- O Replicating vesicular stomatitis virus (VSV) pseudovirus generation
- Pseudovirus infection assay using replicating VSV pseudovirus
- O In vitro viral entry inhibition experiments
- QUANTIFICATION AND STATISTICAL ANALYSIS
- ADDITIONAL RESOURCES

#### SUPPLEMENTAL INFORMATION

Supplemental information can be found online at https://doi.org/10.1016/j. crmeth.2023.100503.

#### **ACKNOWLEDGMENTS**

This work was supported by the National Institutes of Health (GM007365 and GM145402 to H.C.C., GM102365 to R.B.A., LM013337 to Y.L., GM141627 and HG011316 to L.C.), by the Donald and Delia Baxter Foundation (to L.C.), by the National Science Foundation (1953686 to M.W.), by the Knight-Hennessy Scholarships (to H.C.C.), and by a kind gift from the Weintz Family (to L.C.). The funding bodies had no role in the design of the study and collection, analysis, and interpretation of data or in writing the manuscript. Figure 1 and the graphical abstract were created using BioRender.

### **AUTHOR CONTRIBUTIONS**

Conceptualization, H.C.C., L.C., and R.B.A.; methodology, H.C.C., A.S.K., C.W., Y.Q., J.Z., J.C., and L.C.; software, H.C.C. and A.S.K.; formal analysis, H.C.C., A.S.K., and L.C.; investigation, H.C.C., A.S.K., C.W., Y.Q., and J.Z.; resources, R.B.A., Y.L., and L.C.; writing - original draft, H.C.C., A.S.K., R.B.A., and L.C.; writing - review & editing, H.C.C., A.S.K., and L.C.; supervision, J.C., M.W., R.B.A., Y.L., and L.C.

### **DECLARATION OF INTERESTS**

The authors declare no competing interests.

# **INCLUSION AND DIVERSITY**

We worked to ensure gender balance in the recruitment of human subjects. We worked to ensure ethnic or other types of diversity in the recruitment of human subjects. We worked to ensure diversity in experimental samples through the selection of the cell lines. One or more of the authors of this paper self-identifies as an underrepresented ethnic minority in their field of research or within their geographical location. One or more of the authors of this paper self-identifies as a gender minority in their field of research.

Received: November 4, 2022 Revised: April 1, 2023 Accepted: May 23, 2023 Published: May 29, 2023

### REFERENCES

- 1. Shang, J., Wan, Y., Luo, C., Ye, G., Geng, Q., Auerbach, A., and Li, F. (2020). Cell entry mechanisms of SARS-CoV-2. Proc. Natl. Acad. Sci. USA 117, 11727-11734. https://doi.org/10.1073/PNAS.2003138117.
- 2. Hoffmann, M., Kleine-Weber, H., Schroeder, S., Krüger, N., Herrler, T., Erichsen, S., Schiergens, T.S., Herrler, G., Wu, N.H., Nitsche, A., et al. (2020). SARS-CoV-2 cell entry depends on ACE2 and TMPRSS2 and is blocked by a clinically proven protease inhibitor. Cell 181, 271-280.e8. https://doi.org/10.1016/J.CELL.2020.02.052.

- 3. Daly, J.L., Simonetti, B., Klein, K., Chen, K.E., Williamson, M.K., Antón-Plágaro, C., Shoemark, D.K., Simón-Gracia, L., Bauer, M., Hollandi, R., et al. (2020). Neuropilin-1 is a host factor for SARS-CoV-2 infection. Science 370, 861-865. https://doi.org/10.1126/SCIENCE.ABD3072.
- 4. Muus, C., Luecken, M.D., Eraslan, G., Sikkema, L., Waghray, A., Heimberg, G., Kobayashi, Y., Vaishnav, E.D., Subramanian, A., Smillie, C., et al. (2021). Single-cell meta-analysis of SARS-CoV-2 entry genes across tissues and demographics. Nat. Med. 27, 546-559. https://doi.org/10. 1038/s41591-020-01227-z.
- 5. Sungnak, W., Huang, N., Bécavin, C., Berg, M., Queen, R., Litvinukova, M., Talavera-López, C., Maatz, H., Reichart, D., Sampaziotis, F., et al. (2020). SARS-CoV-2 entry factors are highly expressed in nasal epithelial cells together with innate immune genes. Nat. Med. 26, 681-687. https:// doi.org/10.1038/s41591-020-0868-6.
- 6. Ravindra, N.G., Alfajaro, M.M., Gasque, V., Huston, N.C., Wan, H., Szigeti-Buck, K., Yasumoto, Y., Greaney, A.M., Habet, V., Chow, R.D., et al. (2021). Single-cell longitudinal analysis of SARS-CoV-2 infection in human airway epithelium identifies target cells, alterations in gene expression, and cell state changes. PLoS Biol. 19, e3001143. https://doi.org/10. 1371/JOURNAL.PBIO.3001143.
- 7. Horowitz, J.E., Kosmicki, J.A., Damask, A., Sharma, D., Roberts, G.H.L., Justice, A.E., Banerjee, N., Coignet, M.V., Yadav, A., Leader, J.B., et al. (2022). Genome-wide analysis provides genetic evidence that ACE2 influences COVID-19 risk and yields risk scores associated with severe disease. Nat. Genet. 54, 382-392. https://doi.org/10.1038/S41588-021-01006-7
- 8. Reis, G., dos Santos Moreira-Silva, E.A., Silva, D.C.M., Thabane, L., Milagres, A.C., Ferreira, T.S., dos Santos, C.V.Q., de Souza Campos, V.H., Nogueira, A.M.R., de Almeida, A.P.F.G., et al. (2022). Effect of early treatment with fluvoxamine on risk of emergency care and hospitalisation among patients with COVID-19: the TOGETHER randomised, platform clinical trial. Lancet. Glob. Health 10, e42-e51. https://doi.org/10.1016/ S2214-109X(21)00448-4.
- 9. Li, Y., Yang, X., Yan, P., Sun, T., Zeng, Z., and Li, S. (2021). Metformin in patients with COVID-19: a systematic Review and meta-analysis. Front. Med. 8, 704666. https://doi.org/10.3389/FMED.2021.704666.
- 10. The RECOVERY Collaborative Group (2021). Dexamethasone in hospitalized patients with covid-19 - preliminary report. N. Engl. J. Med. 384, 693-704. https://doi.org/10.1056/NEJMOA2021436.
- 11. Takashita, E., Kinoshita, N., Yamayoshi, S., Sakai-Tagawa, Y., Fujisaki, S., Ito, M., Iwatsuki-Horimoto, K., Chiba, S., Halfmann, P., Nagai, H., et al. (2022). Efficacy of antibodies and antiviral drugs against covid-19 omicron variant. N. Engl. J. Med. 386, 995-998. https://doi.org/10. 1056/NFJMC2119407
- 12. VanBlargan, L.A., Errico, J.M., Halfmann, P.J., Zost, S.J., Crowe, J.E., Purcell, L.A., Kawaoka, Y., Corti, D., Fremont, D.H., and Diamond, M.S. (2022). An infectious SARS-CoV-2 B.1.1.529 Omicron virus escapes neutralization by therapeutic monoclonal antibodies. Nat. Med. 28, 490-495. https://doi.org/10.1038/S41591-021-01678-Y.
- 13. Arora, P., Zhang, L., Rocha, C., Sidarovich, A., Kempf, A., Schulz, S., Cossmann, A., Manger, B., Baier, E., Tampe, B., et al. (2022). Comparable neutralisation evasion of SARS-CoV-2 omicron subvariants BA.1, BA.2, and BA.3. Lancet Infect. Dis. 22, 766-767. https://doi.org/10.1016/ S1473-3099(22)00224-9.
- 14. Mannar, D., Saville, J.W., Zhu, X., Srivastava, S.S., Berezuk, A.M., Tuttle, K.S., Marquez, A.C., Sekirov, I., and Subramaniam, S. (2022). SARS-CoV-2 Omicron variant: antibody evasion and cryo-EM structure of spike protein-ACE2 complex. Science 375, 760-764. https://doi.org/10.1126/SCI-
- 15. Meng, B., Abdullahi, A., Ferreira, I.A.T.M., Goonawardane, N., Saito, A., Kimura, I., Yamasoba, D., Gerber, P.P., Fatihi, S., Rathore, S., et al. (2022). Altered TMPRSS2 usage by SARS-CoV-2 Omicron impacts infectivity and fusogenicity. Nature 603, 706-714. https://doi.org/10.1038/ s41586-022-04474-x.

# Report



- 16. Lobritz, M.A., Ratcliff, A.N., and Arts, E.J. (2010). HIV-1 entry, inhibitors, and resistance. Viruses 2, 1069-1105. https://doi.org/10.3390/V2051069.
- 17. Velavan, T.P., Pallerla, S.R., Rüter, J., Augustin, Y., Kremsner, P.G., Krishna, S., and Meyer, C.G. (2021). Host genetic factors determining COVID-19 susceptibility and severity. EBioMedicine 72, 103629. https:// doi.org/10.1016/J.EBIOM.2021.103629.
- 18. Schneider, W.M., Luna, J.M., Hoffmann, H.H., Sánchez-Rivera, F.J., Leal, A.A., Ashbrook, A.W., Le Pen, J., Ricardo-Lax, I., Michailidis, E., Peace, A., et al. (2021). Genome-scale identification of SARS-CoV-2 and pan-coronavirus host factor networks. Cell 184, 120-132.e14. https://doi.org/10. 1016/J.CELL.2020.12.006.
- 19. Wang, R., Simoneau, C.R., Kulsuptrakul, J., Bouhaddou, M., Travisano, K.A., Hayashi, J.M., Carlson-Stevermer, J., Zengel, J.R., Richards, C.M., Fozouni, P., et al. (2021). Genetic screens identify host factors for SARS-CoV-2 and common cold coronaviruses. Cell 184, 106-119.e14. https://doi.org/10.1016/J.CELL.2020.12.004.
- 20. Daniloski, Z., Jordan, T.X., Wessels, H.H., Hoagland, D.A., Kasela, S., Legut, M., Maniatis, S., Mimitou, E.P., Lu, L., Geller, E., et al. (2021). Identification of required host factors for SARS-CoV-2 infection in human cells. Cell 184, 92-105.e16. https://doi.org/10.1016/J.CELL.2020.10.030.
- 21. Baggen, J., Persoons, L., Vanstreels, E., Jansen, S., Van Looveren, D., Boeckx, B., Geudens, V., De Man, J., Jochmans, D., Wauters, J., et al. (2021). Genome-wide CRISPR screening identifies TMEM106B as a proviral host factor for SARS-CoV-2. Nat. Genet. 53, 435-444. https://doi. ora/10.1038/S41588-021-00805-2.
- 22. Zhu, Y., Feng, F., Hu, G., Wang, Y., Yu, Y., Zhu, Y., Xu, W., Cai, X., Sun, Z., Han, W., et al. (2021). A genome-wide CRISPR screen identifies host factors that regulate SARS-CoV-2 entry. Nat. Commun. 12, 961. https://doi. org/10.1038/s41467-021-21213-4.
- 23. Rebendenne, A., Roy, P., Bonaventure, B., Chaves Valadão, A.L., Desmarets, L., Arnaud-Arnould, M., Rouillé, Y., Tauziet, M., Giovannini, D., Touhami, J., et al. (2022). Bidirectional genome-wide CRISPR screens reveal host factors regulating SARS-CoV-2, MERS-CoV and seasonal HCoVs. Nat. Genet. 54, 1090-1102. https://doi.org/10.1038/s41588-022-01110-2.
- 24. Biering, S.B., Sarnik, S.A., Wang, E., Zengel, J.R., Leist, S.R., Schäfer, A., Sathyan, V., Hawkins, P., Okuda, K., Tau, C., et al. (2022). Genome-wide bidirectional CRISPR screens identify mucins as host factors modulating SARS-CoV-2 infection. Nat. Genet. 54, 1078-1089. https://doi.org/10. 1038/s41588-022-01131-x.
- 25. Zhu, S., Liu, Y., Zhou, Z., Zhang, Z., Xiao, X., Liu, Z., Chen, A., Dong, X., Tian, F., Chen, S., et al. (2022). Genome-wide CRISPR activation screen identifies candidate receptors for SARS-CoV-2 entry. Sci. China Life Sci. 65, 701-717. https://doi.org/10.1007/S11427-021-1990-5.
- 26. Bock, C., Datlinger, P., Chardon, F., Coelho, M.A., Dong, M.B., Lawson, K.A., Lu, T., Maroc, L., Norman, T.M., Song, B., et al. (2022). High-content CRISPR screening. Nat. Rev. Methods Primers 2, 8. https://doi.org/10. 1038/s43586-021-00093-4.
- 27. Kim, S.Y., Jin, W., Sood, A., Montgomery, D.W., Grant, O.C., Fuster, M.M., Fu, L., Dordick, J.S., Woods, R.J., Zhang, F., and Linhardt, R.J. (2020). Characterization of heparin and severe acute respiratory syndromerelated coronavirus 2 (SARS-CoV-2) spike glycoprotein binding interactions. Antiviral Res. 181, 104873. https://doi.org/10.1016/J.ANTIVIRAL.
- 28. Lalau, J.D., Al-Salameh, A., Hadjadj, S., Goronflot, T., Wiernsperger, N., Pichelin, M., Allix, I., Amadou, C., Bourron, O., Duriez, T., et al. (2021), Metformin use is associated with a reduced risk of mortality in patients with diabetes hospitalised for COVID-19. Diabetes Metab. 47, 101216. https://doi.org/10.1016/J.DIABET.2020.101216.
- 29. Luo, P., Qiu, L., Liu, Y., Liu, X.L., Zheng, J.L., Xue, H.Y., Liu, W.H., Liu, D., and Li, J. (2020). Metformin treatment was associated with decreased mortality in COVID-19 patients with diabetes in a retrospective analysis. Am. J. Trop. Med. Hyg. 103, 69-72. https://doi.org/10.4269/AJTMH.20-0375.

- 30. Crouse, A.B., Grimes, T., Li, P., Might, M., Ovalle, F., and Shalev, A. (2021). Metformin use is associated with reduced mortality in a diverse population with COVID-19 and diabetes. Front. Endocrinol. 11, 1081. https://doi.org/ 10.3389/FENDO.2020.600439.
- 31. Bramante, C.T., Huling, J.D., Tignanelli, C.J., Buse, J.B., Liebovitz, D.M., Nicklas, J.M., Cohen, K., Puskarich, M.A., Belani, H.K., Proper, J.L., et al. (2022). Randomized trial of metformin, ivermectin, and fluvoxamine for covid-19. N. Engl. J. Med. 387, 599-610. https://doi.org/10.1056/ NEJMOA2201662.
- 32. Polishchuk, P. (2017). Interpretation of quantitative structure-activity relationship models: past, present, and future. J. Chem. Inf. Model. 57, 2618-2639. https://doi.org/10.1021/ACS.JCIM.7B00274.
- 33. Keiser, M.J., Roth, B.L., Armbruster, B.N., Ernsberger, P., Irwin, J.J., and Shoichet, B.K. (2007). Relating protein pharmacology by ligand chemistry. Nat. Biotechnol. 25, 197-206. https://doi.org/10.1038/nbt1284.
- 34. Subramanian, A., Tamayo, P., Mootha, V.K., Mukherjee, S., Ebert, B.L., Gillette, M.A., Paulovich, A., Pomeroy, S.L., Golub, T.R., Lander, E.S., and Mesirov, J.P. (2005). Gene set enrichment analysis: a knowledge-based approach for interpreting genome-wide expression profiles. Proc. Natl. Acad. Sci. 102, 15545-15550. https://doi.org/10.1073/PNAS.0506580102.
- 35. Cousins, H., Hall, T., Guo, Y., Tso, L., Tzeng, K.T.H., Cong, L., and Altman, R.B. (2023). Gene set proximity analysis: expanding gene set enrichment analysis through learned geometric embeddings, with drug-repurposing applications in COVID-19. Bioinformatics 39, btac735. https://doi.org/ 10.1093/BIOINFORMATICS/BTAC735.
- 36. Wilcox, C.S., and Pitt, B. (2020). Is spironolactone the preferred reninangiotensin-aldosterone inhibitor for protection against COVID-19? J. Cardiovasc. Pharmacol. 77, 323-331. https://doi.org/10.1097/FJC. 0000000000000960.
- 37. Rahmani, W., Chung, H., Sinha, S., Bui-Marinos, M.P., Arora, R., Jaffer, A., Corcoran, J.A., Biernaskie, J., and Chun, J. (2022). Attenuation of SARS-CoV-2 infection by losartan in human kidney organoids. iScience 25, 103818. https://doi.org/10.1016/J.ISCI.2022.103818.
- 38. Dong, D., Fan, T.T., Ji, Y.S., Yu, J.Y., Wu, S., and Zhang, L. (2019). Spironolactone alleviates diabetic nephropathy through promoting autophagy in podocytes. Int. Urol. Nephrol. 51, 755-764. https://doi.org/10.1007/ S11255-019-02074-9.
- 39. Keidar, S., Gamliel-Lazarovich, A., Kaplan, M., Pavlotzky, E., Hamoud, S., Hayek, T., Karry, R., and Abassi, Z. (2005). Mineralocorticoid receptor blocker increases angiotensin-converting enzyme 2 activity in congestive heart failure patients. Circ. Res. 97, 946–953. https://doi.org/10.1161/01. RES.0000187500.24964.7A.
- 40. Yeung, M.L., Teng, J.L.L., Jia, L., Zhang, C., Huang, C., Cai, J.P., Zhou, R., Chan, K.H., Zhao, H., Zhu, L., et al. (2021). Soluble ACE2-mediated cell entry of SARS-CoV-2 via interaction with proteins related to the renin-angiotensin system. Cell 184, 2212-2228.e12. https://doi.org/10.1016/J.CELL. 2021.02.053.
- 41. Tomlins, S.A., Rhodes, D.R., Perner, S., Dhanasekaran, S.M., Mehra, R., Sun, X.W., Varambally, S., Cao, X., Tchinda, J., Kuefer, R., et al. (2005). Recurrent fusion of TMPRSS2 and ETS transcription factor genes in prostate cancer. Science 310, 644-648. https://doi.org/10.1126/SCIENCE.
- 42. Di Filippo, L., Formenti, A.M., Rovere-Querini, P., Carlucci, M., Conte, C., Ciceri, F., Zangrillo, A., and Giustina, A. (2020). Hypocalcemia is highly prevalent and predicts hospitalization in patients with COVID-19. Endocrine 68, 475-478. https://doi.org/10.1007/S12020-020-02383-5.
- 43. Alfano, G., Ferrari, A., Fontana, F., Perrone, R., Mori, G., Ascione, E., Magistroni, R., Venturi, G., Pederzoli, S., Margiotta, G., et al. (2021). Hypokalemia in patients with COVID-19. Clin. Exp. Nephrol. 25, 401-409. https:// doi.org/10.1007/S10157-020-01996-4.
- 44. Abbasi, F., Adatorwovor, R., Davarpanah, M.A., Mansoori, Y., Hajiani, M., Azodi, F., Sefidbakht, S., Davoudi, S., Rezaei, F., Mohammadmoradi, S., and Asadipooya, K. (2022). A randomized trial of sitagliptin and



- spironolactone with combination therapy in hospitalized adults with COVID-19. J. Endocr. Soc. 6, bvac017. https://doi.org/10.1210/ JENDSO/BVAC017.
- 45. Kotfis, K., Karolak, I., Lechowicz, K., Zegan-Barańska, M., Pikulska, A., Niedźwiedzka-Rystwej, P., Kawa, M., Sieńko, J., Szylińska, A., and Wiśniewska, M. (2022). Mineralocorticoid receptor antagonist (potassium canrenoate) does not influence outcome in the treatment of COVID-19associated pneumonia and fibrosis-A randomized placebo controlled clinical trial. Pharmaceuticals 15, 200. https://doi.org/10.3390/ph15020200.
- 46. Gordon, D.E., Hiatt, J., Bouhaddou, M., Rezelj, V.V., Ulferts, S., Braberg, H., Jureka, A.S., Obernier, K., Guo, J.Z., Batra, J., et al. (2020). Comparative host-coronavirus protein interaction networks reveal pan-viral disease mechanisms. Science, 370. https://doi.org/10.1126/SCIENCE.ABE9403.
- 47. Zhou, Y., Liu, Y., Gupta, S., Paramo, M.I., Hou, Y., Mao, C., Luo, Y., Judd, J., Wierbowski, S., Bertolotti, M., et al. (2022). A comprehensive SARS-CoV-2-human protein-protein interactome reveals COVID-19 pathobiology and potential host therapeutic targets. Nat. Biotechnol. 41. 128-139. https://doi.org/10.1038/s41587-022-01474-0.
- 48. Grant, S.N., and Lester, H.A. (2021). Regulation of epithelial sodium channel activity by SARS-CoV-1 and SARS-CoV-2 proteins. Biophys. J. 120, 2805-2813. https://doi.org/10.1016/J.BPJ.2021.06.005.
- 49. Wang, C., Dinesh, R.K., Qu, Y., Rustagi, A., Cousins, H., Zengel, J., Guo, Y., Hall, T., Beck, A., Tso, L., et al. (2021). CRISPRa screening with real world evidence identifies potassium channels as neuronal entry factors and druggable targets for SARS-CoV-2. Preprint at bioRxiv. https://doi. org/10.1101/2021.07.01.450475.
- 50. Dieterle, M.E., Haslwanter, D., Bortz, R.H., Wirchnianski, A.S., Lasso, G., Vergnolle, O., Abbasi, S.A., Fels, J.M., Laudermilch, E., Florez, C., et al. (2020). A replication-competent vesicular stomatitis virus for studies of

- SARS-CoV-2 spike-mediated cell entry and its inhibition. Cell Host Microbe 28, 486-496.e6. https://doi.org/10.1016/j.chom.2020.06.020.
- 51. Kanehisa, M., Furumichi, M., Tanabe, M., Sato, Y., and Morishima, K. (2017). KEGG: new perspectives on genomes, pathways, diseases and drugs. Nucleic Acids Res. 45, D353-D361. https://doi.org/10.1093/NAR/ GKW1092.
- 52. Wishart, D.S., Knox, C., Guo, A.C., Cheng, D., Shrivastava, S., Tzur, D., Gautam, B., and Hassanali, M. (2008). DrugBank: a knowledgebase for drugs, drug actions and drug targets. Nucleic Acids Res. 36, D901-D906. https://doi.org/10.1093/NAR/GKM958.
- 53. Stanford SNAP Group (2017). MINER: Gigascale Multimodal Biological Network.
- 54. Charlson, M.E., Pompei, P., Ales, K.L., and MacKenzie, C.R. (1987). A new method of classifying prognostic comorbidity in longitudinal studies: development and validation. J. Chronic Dis. 40, 373-383. https://doi. org/10.1016/0021-9681(87)90171-8.
- 55. Klein, A., and Luo, Y. (2022). PsmPy: a package for retrospective cohort matching in Python. In Annual International Conference of the IEEE Engineering in Medicine & Biology Society (EMBC), pp. 1354-1357. https://doi. org/10.1109/EMBC48229.2022.9871333.
- 56. Austin, P.C. (2011). An introduction to propensity score methods for reducing the effects of confounding in observational studies. Multivariate Behav. Res. 46, 399-424. https://doi.org/10.1080/00273171.2011.568786.
- 57. Beier, K.T., Saunders, A., Oldenburg, I.A., Miyamichi, K., Akhtar, N., Luo, L., Whelan, S.P.J., Sabatini, B., and Cepko, C.L. (2011). Anterograde or retrograde transsynaptic labeling of CNS neurons with vesicular stomatitis virus vectors. Proc. Natl. Acad. Sci. USA 108, 15414-15419. https://doi. org/10.1073/pnas.1110854108.





# **STAR**\*METHODS

#### **KEY RESOURCES TABLE**

REAGENT or RESOURCE	SOURCE	IDENTIFIER
Bacterial and virus strains		
VSVdG-GFP-CoV2-S	Dieterle, et al. <sup>50</sup>	https://doi.org/10.1016/j.chom.2020.06.020.
VSVdG-RABV-G SAD-B19	Dieterle, et al. <sup>50</sup>	https://doi.org/10.1016/j.chom.2020.06.020.
Chemicals, peptides, and recombinant pr	roteins	
Poly-D-Lysine	Thermo Fisher	Cat# A3890401
Spironolactone	Sigma Aldrich	Cat# S3378
SARS-CoV-2 S	GenBank	Cat# MN908947.3
Critical commercial assays		
Incucyte	Sartorius	Cat# 4647
Deposited data		
Schneider CRISPR screen	Schneider et al. 18	GEO: GSE162038
Wang CRISPR screen	Wang et al. <sup>19</sup>	EMBL-EBI ArrayExpress: E-MTAB-9638
Daniloski CRISPR screen	Daniloski et al. <sup>20</sup>	GEO: GSE158298
Baggen CRISPR screen	Baggen et al. <sup>21</sup>	NCBI BioProject: PRJNA685335
Zhu Y CRISPR screen	Zhu Y et al. <sup>22</sup>	https://doi.org/10.1038/s41467-021-21213-4
Rebendenne CRISPR screen	Rebendenne et al. <sup>23</sup>	GEO: GSE175666
Biering CRISPR screen	Biering et al. <sup>24</sup>	https://doi.org/10.1038/s41588-022-01131-x
Zhu S CRISPR screen	Zhu S et al. <sup>25</sup>	https://doi.org/10.1007/s11427-021-1990-5
Experimental models: Cell lines		
A549-ACE2 cell line	This study	N/A
HEK293T-ACE2 cell line	This study	N/A
VeroE6	ATCC	# CRL-1586
Recombinant DNA		
pLenti-ACE2	Addgene	Plasmid #202533
VSV-eGFP-dG	Addgene	Plasmid #31842
Software and algorithms		
RxGRID	This study	https://doi.org/10.5281/zenodo.7789897

# **RESOURCE AVAILABILITY**

# **Lead contact**

Further information and requests for resources and reagents should be directed to and will be fulfilled by the lead contact, Le Cong (congle@stanford.edu).

# **Materials availability**

Plasmid used to generate the ACE2 cell lines in this study (pLenti-EF1A-hACE2-2A-Puro) has been deposited to Addgene for open distribution, with plasmid ID: 202533.

# **Data and code availability**

All CRISPR screening data analyzed are publicly available from their respective source publications as listed in the key resources table. Patient medical record data is not publicly available due to patient privacy regulations. Pseudoviral inhibition assay data will be shared by the lead contact upon request.

All original code has been deposited at https://github.com/henrycousins/RxGRID and archived on Zenodo (https://doi.org/10. 5281/zenodo.7789897) and is publicly available as of the date of publication.

Any additional information required to reanalyze the data reported in this paper is available from the lead contact upon request.



# **EXPERIMENTAL MODEL AND STUDY PARTICIPANT DETAILS**

#### Cell lines

A549-ACE2 or HEK293T-ACE2 cells were used in the current study. For both A549-ACE2 and HEK293T-ACE2 cells, the cells were originally obtained from the American type culture collection (ATCC). All cells were cultured in Dulbecco's Modified Eagle Medium (DMEM) with 10% Fetal Bovine Serum (FBS, Thermo Fisher Scientific). Cells were cultured at 37°C and in 5% CO2 incubator. According to supplier, A549-ACE2 cells were isolated from the lung tissue of a male with lung cancer. The HEK293T-ACE2 cells were derived from human embryonic kidney cells grown in tissue culture taken from a female. All cells were authenticated by the supplier and double checked via STR analysis performed by American type culture collection (ATCC).

### **Medical records**

Patient medical records were obtained from the Northwestern Medicine Electronic Data Warehouse. Summaries of the cohort definition and characteristics are available in Figures 4 and S3, respectively. The investigation comprised 1,462 patients (72.1% [1,054] female, 27.9% [408] male) with a mean age of 55.4 (standard deviation 20.7) years. Ethical approval was obtained from the Northwestern University IRB (STU00212845) prior to initiation of the study.

#### **METHOD DETAILS**

# **CRISPR** screening data

We identified published, genome-wide CRISPR-KO (loss-of-function) screens of SARS-CoV-2 entry in human cells available as of May 2022, with five screens meeting criteria. Three screens were performed in HuH-7 liver cells, and two were performed in A549 lung epithelial cells. Multiplicities of infection (MOI) for each screen ranged from 0.01 to 3. We also identified genome-wide CRISPRa (increase-of-expression) screens in human cells available as of May 2022, with three screens meeting criteria. These included two screens in Calu-3 lung epithelial cells and one in HEK293T embryonic kidney cells, with MOI ranging from 0.005 to 0.5. Raw data for each screen was obtained from the respective source publication.

### **Functional enrichment analysis**

Enrichment analyses were performed using the prerank gene set enrichment analysis (GSEA) algorithm using the default runtime parameters, using Kyoto Encyclopedia of Genes and Genomes (KEGG) pathway gene sets. 51 We defined significance as a false discovery rate (FDR) less than 0.05.

# **Network-based drug rankings**

Drug-gene interactions for known drugs from DrugBank were used to construct a bipartite graph G = (V, E), with the set of nodes Vrepresenting either drugs or genes and the set of edges E representing known interactions between protein-coding genes and drugs. 52,53 The complete network contained 7,233 nodes (4,927 compounds and 2,306 genes) and 14,863 edges.

For each screen, a unique subgraph  $g_k = (V_{k0} E_k)$  encompassing only screen-specific genetic hits was defined. Equivalently,

$$V_k = \{v | v \in H_k\} \cup \{v | v \in D_k\}$$

where  $H_k$  is the set of hit genes from screen k (top 5% by default) in the network, and  $D_k$  is the set of drugs connected to at least one gene in  $H_k$ .

In each subgraph  $g_k$ , compounds were ranked by normalized degree centrality, defined as node degree normalized to the total number of possible neighbors ( $NDC_n = \text{degree}(v_n)/|H_k|$ ), reflecting each compound's proximity to host entry factors identified in the screen. Alternative measures of centrality, including betweenness centrality and eigenvector centrality, were also evaluated. Their agreement with degree centrality rankings was assessed by Spearman correlation owing to non-normality.

Aggregation of screen-specific results into a final ranking was done was performed by computing the intersection of screen-specific drug hits, reasoning that this method better accommodates screen-level variability than does mean or median pooling. Specifically, we defined the set of screen-specific drug hits Rk as the top 1% of compounds by degree centrality for each screen k and ranked drugs by the frequency at which they were a hit in any screen. Equivalently,

$$rank_j = \sum_{K} \mathbf{1} \big\{ v_j \in R_k \big\}$$

where  $R_k$  is the set of screen-specific drug hits for screen k. We selected for follow-up all drugs identified as hits in at least one-third of all screens, excluding narcotics, anesthetics, and dietary supplements.

# **Cohort construction**

De-identified patient medical records were obtained from the Northwestern Medicine Electronic Data Warehouse. Records were filtered to include only patients who had a positive COVID-19 test by means of reverse transcription-polymerase chain reaction (RT-PCR) testing. Patients who had more than one positive test were sorted by date, and the first was selected to create a unique



set of patient identifiers. A 6-month time window preceding the first positive COVID-19 test was created for use as a filter for medication treatment status.

Patient characteristics that served as covariates considered in the analysis included race, gender, age, postal code, and medical comorbidities such as hypertension, diabetes, metastatic cancer, rheumatological disease, autoimmune disorders, and kidney failure, which are reported according to Charlson Comorbidities.<sup>54</sup> The full list of comorbidities is provided as supplementary material (Figure S3). Records in which both race and postal code were missing (n = 8,201) were removed, as data was not missing at random. The final database included 64,349 unique patients with a positive COVID-19 test and complete comorbidity labels.

For each of the medications under investigation, treatment groups were identified by string matching to generic/brand names for the medication of interest. We defined users as those with medication orders occurring within 6 months preceding their first recorded COVID-19-positive specimen, such that treatment status connotes drug exposure prior to COVID-19 diagnosis.

In addition to the candidate drugs from RxGRID, we also analyzed metformin as a widely prescribed comparator drug with a well-documented association with COVID-19 outcomes. Specifically, metformin use has been associated with reduced COVID-19 severity in at least 8 separate observational studies, as well as in a meta-analysis of 19 observational studies, which found an aggregate OR of 0.73 for hospitalization. Furthermore, the COVID-OUT randomized controlled trial identified a protective effect (OR 0.58) for metformin against emergency department visit, hospitalization, or death in a secondary analysis. 31

# **Propensity score matching**

Propensity score matching was performed using the *psmpy* package in Python 3.7.<sup>55</sup> In our use case, logistic regression was executed where the treatment state (for the medication of interest) was regressed on the set of covariates defined previously. Due to the size imbalance between treatment and control group sizes, logistic regression was run repeatedly on a balanced sample to generate a probability integer for each observation by folding iteratively over the larger class and averaging over repeated patient indexes. The logit of the logistic regression prediction was calculated for control and treatment observations, as it more closely approximates a normal distribution.<sup>56</sup> Following this, a unidimensional k-nearest neighbors (k-NN) algorithm was fitted to the logit scores of the control group. The treatment group was then fitted to the model, calculating Euclidean distance as the similarity metric. Am exclusionary caliper size of 0.25 of the standard deviation of the distance was implemented to reduce distant matches. To prevent samples from sharing the closest first match, matching was performed without replacement. In this way, treatment-control patient pairs were identified in which each subject had an approximate equal likelihood of receiving the drug of interest.

To verify adequate matching, a Cohen's D statistic (standardized mean difference) was calculated before and after matching, ensuring that the matched cohort had smaller covariate effect sizes. Additionally, the two cohorts' logit scores and the number of patients in each category were compared to confirm similarity.

### **Software**

Computational analyses were performed in a Python 3.7 environment using NetworkX 2.2, NumPy 1.21.6, pandas 1.2.3, Matplotlib 3.5.3, and seaborn 0.12.2, in addition to the standard Python library.

# Replicating vesicular stomatitis virus (VSV) pseudovirus generation

Recombinant VSV expressing eGFP (VSVdG-GFP-CoV2-S) was generated using plasmid-based methods. The plasmid to rescue this virus was generated by inserting a codon optimized SARS-CoV2-S based on the Wuhan-Hu-1 isolate (GenBank:MN908947.3), which was mutated to remove a putative ER retention domain (K1269A and H1271A) into a VSV-eGFP-dG vector (pVSV eGFP dG was a gift from Connie Cepko, <sup>57</sup> Addgene plasmid # 31842; http://n2t.net/addgene:31842; RRID:Addgene\_31842), in frame with the deleted VSV-G. The control virus VSVdG-RABV-G SAD-B19 was also generated by inserting Rabies virus G in the same vector. Both viruses were rescued in 293FT/VeroE6 cell co-culture and amplified in VeroE6 cells and titrated in VeroE6 cells over-expressing TMPRSS2. Sequencing of the amplified virus revealed an early C-terminal Stop signal (1274STOP) and a partial mutation at A372T (~50%) in the ectodomain, as previously reported. <sup>50</sup>

# Pseudovirus infection assay using replicating VSV pseudovirus

A549-ACE2 or HEK293FT-ACE2 cells were plated in clear 96-well plates at 2x104 cells per well approximately 24 hours prior to infection in 100 uL of media (DMEM) containing 10% FBS. Cells were infected with VSVdG-CoV2-S or VSVdG-RABV-G at an MOI of 0.1. Infection was performed by diluting virus in media without FBS and adding 150 uL of diluted virus per well. After addition of the virus, the plate was spun at 900 x g for 60 minutes at 30°C. Infection was tracked over time using an Incucyte system (Sartorius) in a 37°C and 5% CO2 incubator using 4x magnification and detecting GFP. GFP+ cells were counted using Incucyte Analysis software and data were reported as GFP positive foci per well after normalization to confluence.

### In vitro viral entry inhibition experiments

All inhibitor assays use 96-well plates coated with Poly-D-Lysine (Thermo Fisher, A3890401) at a concentration of 50 ug/mL for 2 hours at room temperature. The plates were then washed with PBS three times, and 1 x 10<sup>4</sup> cells were plated in a final volume of 100 uL of culture media. The next day, 20 uL of media was removed from each well and replaced with a 5X concentration of the inhibitor in culture media at the indicated dilution. The cells were then returned to 37°C. Two hours later, diluted SARS-CoV-2 Spike



pseudotyped lentiviruses (for an ~MOI of 0.05-0.15) were added to each well. Plates were spinfected and assayed as described above. Drugs (Sigma-Aldrich) were diluted in PBS via vigorously vortexing to a concentration of 100 mM prior to dilution in culture media.

# **QUANTIFICATION AND STATISTICAL ANALYSIS**

Clinical outcomes under investigation included admission to the intensive care unit (ICU) and initiation of mechanical ventilation. Odds ratios for each clinical endpoint, with corresponding confidence intervals and p-values, were calculated using McNemar's test for matched treatment-control pairs. Pseudoviral infectivity at specific time points was measured using Student's T-tests, applying Bonferroni's correction for multiple hypothesis testing. In all cases, two-tailed null hypotheses with a significance threshold of 0.05 were used.

# **ADDITIONAL RESOURCES**

RxGRID is available as a command-line Python package with supporting documentation at https://github.com/henrycousins/ RxGRID.